

## Tunneling-induced luminescence from adsorbed organic molecules with submolecular lateral resolution

Germar Hoffmann,\* Laurent Libiouille,<sup>†</sup> and Richard Berndt<sup>‡</sup>

*Institut für Experimentelle und Angewandte Physik, Christian-Albrechts-Universität zu Kiel, D-24098 Kiel, Germany*

(Received 23 January 2002; published 6 June 2002)

Light emission from molecule-covered surfaces in the scanning tunneling microscope has repeatedly been reported with optical contrast occurring on a molecular scale. The role of the molecules in the emission is unclear although molecular fluorescence has been suggested. Here, simultaneous optical spectroscopy and spatial mapping of the emission from single hexa-*tert*-butyl-decacyclene molecules on noble-metal surfaces are combined and submolecular contrast is observed. However, the emission spectra are indicative of plasmon mediated emission of the metal substrate and tip while the molecule merely acts as a spacer, which slightly modifies the plasmon emission.

DOI: 10.1103/PhysRevB.65.212107

PACS number(s): 68.37.Ef, 33.80.-b, 73.21.-b

How to combine the analytical capabilities of optical spectroscopy with subnanometre lateral resolution? One approach to this problem is based on the observation that electron tunneling can lead to the emission of light, as first reported by J. Lambe and S. L. McCarthy for metal-oxide-metal junctions.<sup>1</sup> R. D. Young, having detected electron emission from the topographiner, a precursor of the scanning tunneling microscope (STM), proposed the detection of photons from this device.<sup>2</sup> Following the first experimental observation of light emission from metal and semiconductor surfaces in a STM,<sup>3</sup> a number of reports on light emission from adsorbed molecules appeared.<sup>4–10</sup> Unlike conventional optical spectroscopy STM induced light emission circumvents the spatial limits of classical optics and offers the prospect of addressing a single molecule with nanometre lateral resolution.

Optical contrast in photon maps, i.e., in maps of the photon intensity distribution on a molecular scale has been reported for C<sub>60</sub> on Au(110),<sup>4</sup> copper phthalocyanine on Au(111),<sup>6</sup> octadecylthiol on Au,<sup>7</sup> porphyrin molecules on Cu(100),<sup>8</sup> and alkanethiols on Au(111) (Ref. 9) under varying environmental conditions, i.e., in ultrahigh vacuum, in air, at room temperature, and at cryogenic temperatures. Molecular light emission has also been reported from large-area, squeezable tunnel junctions.<sup>10</sup>

Common to these experimental results is that no direct evidence of molecular fluorescence was available. Given that strong emission is observed from metals even in the absence of molecules<sup>3,11</sup> the interpretation of the emission in terms of a transition that involves molecular states is not a direct one when metal substrates are used. Moreover, radiationless energy transfer from an excited molecular state to the metal substrate is often an efficient decay channel. Therefore the nature of the emission processes from molecule-covered metal surfaces is an open question.

Two STM studies presented additional indications of molecular fluorescence. An observed voltage dependence of fluorescence spectra from porphyrin molecules on Cu(100) led Fujita *et al.* to conclude on “the possible existence of two radiative processes, decay of local surface plasmon and molecular fluorescence.”<sup>8</sup> Based on a deviation of the current dependence of the emission intensity from (partially oxi-

dized) alkanethiols compared to published data from a pristine metal surface<sup>12</sup> the late G. Poirier favored molecular emission.<sup>9</sup> We note in passing that luminescence from poly(*p*-phenylenevinylene) layers on indium-tin oxide has been observed in field emission, i.e., at high bias voltages where the lateral resolution of the STM is rather limited.<sup>13</sup>

While the above results were encouraging, lateral and spectral resolution have not yet been achieved simultaneously which would probably provide more detailed information on the light-emission process. To improve on this state of affairs, we have combined a low-temperature STM with sensitive optical detection.<sup>14</sup> This combination enables STM imaging and simultaneous optical spectroscopy with a spectrum taken at each image point. Moreover, statistically significant spectra can be acquired at relatively low tunneling currents where the adsorbed molecules are not adversely affected. Therefore, spectrally resolved images of *partially* covered surface areas can be recorded, which enables a direct comparison of the emission from the metal and from molecules with the *same STM tip*. Given the known sensitivity of the metal emission to the tip status<sup>15–17</sup> this possibility is essential in obtaining useful data. As a result, some of the interpretational ambiguities of the previous experiments do not occur.

For the organic molecule hexa-*tert*-butyl-decacyclene (HBDC) [Fig. 1(a)] adsorbed on Au(111), Ag(111), and Cu(111) we have achieved submolecular resolution in spectrally resolved maps of the photon intensity. On the molecules the emission is found to be blue shifted as compared to the metal substrate emission. The spectral weights of the emission features are also modified to some extent. However, there is no indication of molecule specific emission. We argue that the molecule-induced modifications of the emission characteristics can qualitatively be understood in terms of the excursion of the STM tip apex as it scans over a molecule. This assignment is corroborated by spectroscopy of the metal fluorescence as a function of the tip-sample distance.

The experiments were performed in a home-built ultrahigh vacuum (UHV) STM,<sup>18</sup> which was operated at a temperature  $T=4.6$  K. The instrument was equipped with optics for spectroscopy of light that is emitted from the tip-sample region.<sup>14</sup> The single-crystal surfaces were cleaned by re-

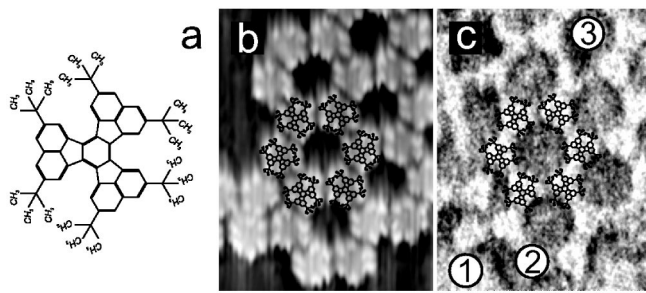


FIG. 1. (a) Molecular structure of hexa-*tert*-butyl-decacyclene with a central decacyclene core and six attached *tert*-butyl legs. (b) Topograph of a HBDC-covered Cu(111) surface with molecules forming superstructures ( $11 \times 8 \text{ nm}^2$ ). (c) Simultaneously acquired photon map ( $I=0.4 \text{ nA}$ ,  $V=2.3 \text{ V}$ ,  $5 \text{ ms/pixel}$ ) with intensity contrast between the clean metal surface (1,  $\approx 8.5 \text{ counts/pC}$ ), on top of molecules (2,  $\approx 10 \text{ counts/pC}$ ) and between molecules (3,  $\approx 3.5 \text{ counts/pC}$ ).

peated sputtering and annealing cycles. HBDC was deposited by evaporation from a heater with the crystals at room temperature in UHV. The deposition rate was controlled by a microbalance and checked afterwards with STM. Ir and W tips were sputtered and annealed in vacuum. While only results of experiments performed at  $\approx 5 \text{ K}$  are shown below, experiments at higher temperatures up to room temperature gave no indication of additional processes. Sample voltages  $|V| < 2.7 \text{ V}$  were used to avoid modification of the molecules which typically occurred at  $V \sim 3 \text{ V}$ .

HBDC was reported to be mobile on Cu(110) (Ref. 19) and Cu(100) (Ref. 20) at room temperature below monolayer coverage. At low temperatures we find stable molecular arrangements although molecular mobility can be induced by the STM tip at elevated currents and voltages. On terraces, HBDC assembles into honeycomb networks as shown in Fig. 1(b). We also observe a more dense hexagonal arrangement in other surface areas [Fig. 1(b), left part]. In agreement with previous room-temperature observations, HBDC appears as a threefold symmetric disk with six bright lobes under the imaging conditions used. The lobes are associated to the *tert*-butyl legs. This assignment is supported by quantum chemistry calculations.<sup>21</sup> For comparison, the experimental data has been overlaid with diagrams of the molecular structure. Figure 1(c) shows photon data, namely, a map of the integral detected photon intensity. Again, the molecular positions as determined from the topograph are indicated. At the relatively low current used ( $I=400 \text{ pA}$ ), the molecular arrangement is stable. Characteristic positions, i.e., on the clean metal surface, on top of a molecule, and between molecules are marked 1–3. In the photon map, individual molecules are clearly resolved as bright spots, the emission being three times more intense on molecules (2) than on the metal

between molecules (3). The emission intensity from the uncovered metal outside the molecular array (1) ( $\approx 8.5 \text{ counts/pC}$ ) is slightly lower than the one from the molecules ( $\approx 10 \text{ counts/pC}$ ).

Similar results are obtained for HBDC molecules adsorbed at steps. Figure 2 displays typical data. HBDC mol-

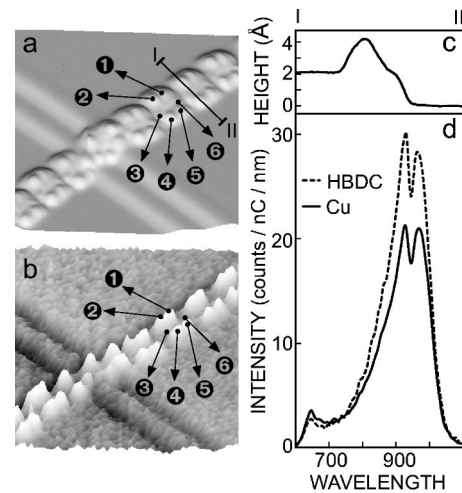


FIG. 2. (a) Topograph of Cu(111) with HBDC molecules decorating steps. (b) Photon map at  $\lambda=921, \dots, 929 \text{ nm}$  with clear intramolecular contrast ( $I=5 \text{ nA}$ ,  $V=2.3 \text{ V}$ ,  $500 \text{ ms/pixel}$ ). (c) Linescan between positions I and II as indicated in the topograph (a). (d) Fluorescence spectra recorded with the STM tip above the metal surface (solid line) and an HBDC molecule (dashed line).

ecules are lining up along a step traversing the image from the bottom left to the upper right corner. In addition to this molecule-covered step, two further, clean ones are discernible. These latter steps are perfectly straight and occur along (110) directions, which is indicative of dislocations. HBDC frequently adsorbs at steps with two *tert*-butyl legs (1,2) located on the upper and four legs on the lower terrace (3–6). The opposite configuration of four and two legs on the upper and lower terraces are observed, too. This tendency of HBDC to make contact to two terraces is similar to the finding of Schunack *et al.*<sup>19</sup> who observed that, on Cu(110), HBDC molecules locally modify the substrate structure as to expose a steplike configuration underneath the molecules. For discussing photon data below, it is important to note that the apparent heights of the *tert*-butyl legs are not identical. Whereas the apparent height of legs 1, 2, 4, and 5 is approximately  $2 \text{ \AA}$  legs 3 and 6 are less clearly discernible.

Fluorescence spectra were recorded from these molecules simultaneously with topographic imaging. Figure 2(b) shows a selected cross-sectional profile of this large, three-dimensional data set, namely, the detected intensity in the wavelength range  $921 \text{ nm} < \lambda < 929 \text{ nm}$ . We notice clear submolecular structure in this photon map, which is associated with the *tert*-butyl legs. Compared to the emission from the Cu terrace, legs 1, 2, 4, and 5 give rise to a 30% increase of the intensity in this wavelength range, similar to the observation from Fig. 1. No clear structure is observed from legs 3 and 6 in the photon map. For completeness, we note that dislocation-related steps affect the photon intensity, presumably via a modified electromagnetic coupling of the tip and the sample.<sup>22–24</sup> The apparent grainy pattern of the terrace emission is caused by statistical variations of the photon numbers in the limited wavelength range under consideration.

The wavelength resolved photon maps shown so far are comparable to previous reports of molecule-related contrast

in maps of the integral photon intensities. Further experimental details become accessible in another representation of the data. Figure 2(d) shows fluorescence spectra of the pristine terrace and from HBDC as measured above a *tert*-butyl leg. The main observation to be made is that the overall shape of the spectra is very similar. Apparently, HBDC does not add any new spectral features to the substrate emission although it does modify the spectral weights to some extent. From a comparison of terrace spectra that were recorded before and after the leg spectrum we exclude artifacts such as unnoticed changes of the tip status. We also verified that all leg spectra are identical within the experimental uncertainty. Before analyzing the molecule-related spectral changes in more detail we briefly discuss the metal emission.

Based on previous experimental and theoretical work,<sup>25,11</sup> a single-peak spectrum may be expected for a W tip on Cu(111), which is typical of a localized, dipolar plasmon. However, an irregular shape of the tip apex can drastically modify the spectral characteristics.<sup>15–17</sup> In the experiment of Fig. 2, an irregular shape was likely to be present because the tip had been cleaned repeatedly by tip-sample collisions to remove molecules from its apex. As a result, in addition to the mode at  $\lambda \sim 600$  nm, a second mode at  $\lambda \sim 950$  nm is resolved. The sharp dip of the intensity at  $\sim 950$  nm is due to the transmission characteristics of the optical fibre used. The sample voltage  $V=2.3$  V causes a short wavelength cutoff of the emission at  $\lambda = hc/eV \sim 540$  nm. As a consequence, the intensity of the shorter wavelength structure at  $\lambda \sim 600$  nm is low. When care is taken to avoid tip-sample collisions the typical W-Cu spectrum is observed (Fig. 3).

Figure 3 shows spectra recorded at identical tunneling parameters ( $V=5$  V,  $I=2.3$  nA) with a different tip. From these spectra the effect of HBDC on the spectrum becomes evident. On the clean copper surface we find an emission maximum at  $\lambda \sim 640$  nm (dashed line), which is indicative of a regular tip shape. While no additional features are observed in the spectrum of HBDC, a 4 nm shift of the HBDC spectrum towards shorter wavelength occurs compared to the substrate spectrum.

Summarizing the experimental data we note that HBDC does not induce new spectral features. However, in the investigated range of sample biases ( $\pm 2.7$  V), it leads to a spectral blue shift of a few nm. This occurs at those positions where HBDC appears as a protrusion in topographs. These findings indicate that the role of the molecule is to modify the tip-induced plasmon by changing the distance of the tip and the metal substrate.

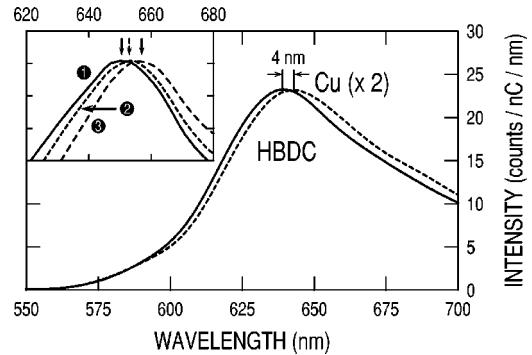


FIG. 3. Fluorescence spectra from HBDC and the surrounding metal surface acquired with a different tip ( $I=5$  nA,  $V=2.3$  V). Spectra are scaled to same intensity as indicated revealing a blue shift of the emission on HBDC. The inset shows three spectra from Au(111) recorded at different currents, i.e., different distances. Spectrum (1) was recorded at  $V=3$  V and  $I=0.3$  nA. Spectrum (2) at  $I=2.8$  nA is red shifted by  $\Delta\lambda=2$  nm, spectrum (3) at  $I=33.7$  nA is shifted further with  $\Delta\lambda=6$  nm.

To test this idea we performed a series of measurements on a clean Au(111) surface where the tip-sample distance was controllably changed while simultaneously recording fluorescence spectra. Three spectra representing smaller (dashed line) and larger (solid line) tip-sample distances are displayed in the inset of Fig. 3. The spectra have been normalized to equal peak intensities. More relevant for the present purpose is the change of the spectral shape. The 1.9 Å distance increase leads to a 6 nm blue shift of the emission. This shift is indeed expected within the framework of localized plasmon modes.<sup>25</sup> Detailed measurements and modeling of this effect will be discussed elsewhere.<sup>26</sup> The similarity of the observation from clean metals with the case of HBDC molecules is striking.

We conclude that the primary effect of HBDC on the emission spectrum is to cause a spectral shift induced by the modified tip-substrate distance. Moreover, we find that the light-emission intensity can be enhanced by the presence of a molecule. No indications of an additional light-emission process were observed for hexa-*tert*-butyl-decacyclene on noble-metal surfaces.

We thank R. R. Schlittler and J. K. Gimzewski for freely sharing hexa-*tert*-butyl-decacyclene molecules and their knowledge about them with us. We acknowledge financial support from the EU IST-FET project “BUN” and the TMR network “EMIT.”

\*Present address: Institut für Angewandte Physik, University of Hamburg, Germany. Electronic address: ghoffmann@physnet.uni-hamburg.de

†Present address: IPMC, Université de Lausanne, CH-1015 Lausanne, Switzerland.

‡Electronic address: berndt@physik.uni-kiel.de

<sup>1</sup>J. Lambe and S.L. McCarthy, Phys. Rev. Lett. **37**, 923 (1976).

<sup>2</sup>R. Young, Phys. Today **24** (11), 42 (1971).

<sup>3</sup>J.H. Coombs *et al.*, J. Microsc. **152**, 325 (1988).

<sup>4</sup>R. Berndt *et al.*, Science **262**, 1425 (1993).

<sup>5</sup>A.W. McKinnon, M.E. Welland, and S.J.D. Warren, Thin Solid Films **257**, 63 (1995).

<sup>6</sup>I.I. Smolyaninov, Surf. Sci. **364**, 79 (1996).

<sup>7</sup>S. Evoy, F.D. Pardo, P.M.S. John, and H.G. Craighead, J. Vac.

- Sci. Technol. A **15**, 1438 (1997).
- <sup>8</sup>D. Fujita *et al.*, Surf. Sci. **454-456**, 1021 (2000).
- <sup>9</sup>G.E. Poirier, Phys. Rev. Lett. **86**, 83 (2001).
- <sup>10</sup>E. Flaxer, O. Sneh, and O. Cheshnovsky, Science **262**, 2012 (1993).
- <sup>11</sup>R. Berndt, J.K. Gimzewski, and P. Johansson, Phys. Rev. Lett. **67**, 3796 (1991).
- <sup>12</sup>R. Berndt, J.K. Gimzewski, and P. Johansson, Phys. Rev. Lett. **71**, 3493 (1993).
- <sup>13</sup>S.F. Alvarado, W. Rieß, P.F. Seidler, and P. Strohhriegl, Phys. Rev. B **56**, 1269 (1997).
- <sup>14</sup>G. Hoffmann, J. Kröger, and R. Berndt, Rev. Sci. Instrum. **73**, 305 (2002).
- <sup>15</sup>G. Hoffmann, J. Aizpurua, S.P. Apell, and R. Berndt, Surf. Sci. **482-485**, 1159 (2001).
- <sup>16</sup>M. Iwami, Y. Uehara, and S. Ushioda, Jpn. J. Appl. Phys., Part 1 **39**, 4912 (2000).
- <sup>17</sup>Y. Uehara, Y. Suda, S. Ushioda, and K. Takeuchi, Appl. Phys. Lett. **79**, 1718 (2001).
- <sup>18</sup>J. Kliewer, Ph. D. thesis, RWTH Aachen, D-52056 Aachen, Germany, 2000.
- <sup>19</sup>M. Schunack *et al.*, Phys. Rev. Lett. **86**, 456 (2001).
- <sup>20</sup>J.K. Gimzewski *et al.*, Science **281**, 531 (1998).
- <sup>21</sup>C. Chavy, C. Joachim, and A. Altibelli, Chem. Phys. Lett. **214**, 569 (1993).
- <sup>22</sup>R. Berndt and J.K. Gimzewski, Phys. Rev. B **48**, 4746 (1993).
- <sup>23</sup>V. Sivel, R. Coratger, F. Ajustron, and J. Beauvillain, Phys. Rev. B **50**, 5628 (1994).
- <sup>24</sup>G. Hoffmann and R. Berndt, Appl. Phys. A: Mater. Sci. Process. **72**, 173 (2001).
- <sup>25</sup>P. Johansson and R. Monreal, Z. Phys. B: Condens. Matter **84**, 269 (1991).
- <sup>26</sup>J. Aizpurua, G. Hoffmann, P. Apell, and R. Berndt (unpublished).